Detection of C$_2$HD and the D/H ratio on Titan

Athena Coustenis [a,*], Donald E. Jennings [b], Antoine Jolly [c], Yves Bénilan [c], Conor A. Nixon [b,d], Sandrine Vinatier [a], Daniel Gautier [a], Gordon L. Bjoraker [b], Paul N. Romani [b], Ronald C. Carlson [e], F. Michael Flasar [b]

[a] Laboratoire d'Etudes Spatiales et d'Instrumentation en Astrophysique (LESIA), Observatoire de Paris-Meudon, 5, Place Jules Janssen, 92195 Meudon Cedex, France
[b] NASA/Goddard Space Flight Center, Code 693, Greenbelt, MD 20771, USA
[c] LISA, CNRS, Univ. Paris 12 and Paris 7, 94010 Créteil Cedex, France
[d] Department of Astronomy, University of Maryland, College Park, MD 20742, USA
[e] IACS, Catholic University of America, and NASA/Goddard Space Flight Center, Greenbelt, MD 20771, USA

ABSTRACT

We report here the first detection of mono-deuterated acetylene (acetylene-d1, C$_2$HD) in Titan's atmosphere from the presence of two of its emission bands at 678 and 519 cm^{-1} as observed in CIRS spectral averages of nadir and limb observations taken between July 2004 and mid-2007. By using new laboratory spectra for this molecule, we were able to derive its abundance at different locations over Titan's disk. We find the C$_2$HD value ($1.27^{-0.13}_{-0.22} \times 10^{-9}$) to be roughly constant with latitude from the South to about 45° N and then to increase slightly in the North, as is the case for C$_2$H$_2$. Fitting the 678 cm^{-1} ν_5 band simultaneously with the nearby C$_2$H$_2$ 729 cm^{-1} ν_5 band, allows us to infer a D/H ratio in acetylene on Titan with an average of the modal values of $2.09 \pm 0.45 \times 10^{-4}$ from the nadir observations, the uncertainties being mainly due to the vertical profile used for the fit of the acetylene band. Although still subject to significant uncertainty, this D/H ratio appears to be significantly larger than the one derived in methane from the CH$_3$D band (upper limit of 1.5×10^{-4}; Bézard, B., Nixon, C.A., Kleiner, I., Jennings, D.E., 2007. Icarus, 191, 397–400; Coustenis, A., Achterberg, R., Conrath, B., Jennings, D., Marten, A., Gautier, D., Bjoraker, G., Nixon, C., Romani, P., Carlson, R., Flasar, M., Samuelson, R.E., Teanby, N., Irwin, P., Bézard, B., Orton, G., Kunde, V., Abbas, M., Courtin, R., Fouchet, Th., Hubert, A., Lellouch, E., Mondellini, J., Taylor, F.W., Vinatier, S., 2007. Icarus 189, 35–62). From the analysis of limb data we infer D/H values of $9.6^{-4.5}_{-3.1} \times 10^{-5}$ (at 54° S), $2.4^{-0.9}_{-0.7} \times 10^{-4}$ (at 15° S), $2.7^{-0.7}_{-0.6} \times 10^{-4}$ (at 54° N) and $1.9^{-0.7}_{-0.5} \times 10^{-4}$ (at 80° N), which average to a mean value of $1.63 \pm 0.27 \times 10^{-4}$.

© 2008 Elsevier Inc. All rights reserved.

1. Introduction

Our understanding of Titan's atmospheric chemical composition has recently been enhanced by the data returned by the Cassini instruments. Spectra recorded by the Composite Infrared Spectrometer (CIRS) became available during the Titan flybys spanning over three years now since attaining Saturn's orbit (e.g. Flasar et al., 2005; Coustenis et al., 2007; Teanby et al., 2007, 2008; Vinatier et al., 2007a, 2007b; Nixon et al., 2008). The spectra characterize various regions on Titan from 80° S to 80° N with a variety of emission angles. We have studied the emission observed in the CIRS detector arrays (covering the 10–1500 cm^{-1} spectral range with apodized resolutions of 2.54 or 0.53 cm^{-1}, referred to as medium and high resolution in this paper). We have used temperature profiles retrieved from the inversion of the radiance observed

in the methane ν_4 band at 1304 cm^{-1} and a line-by-line radiative transfer code to infer the abundances of the trace constituents and some of their isotopes in Titan's stratosphere (Coustenis et al., 2007).

The composite spectra show several signatures of previously identified molecules: hydrocarbons, nitriles, H$_2$, H$_2$O, CO and CO$_2$. Besides these well-known trace species, a firm detection of benzene (C$_6$H$_6$) was made by CIRS, at 674 cm^{-1}, allowing for the study of its latitudinal variations. No longitudinal variations were found for any of the gases. Information has been retrieved on the meridional variations of the trace constituents and tied to predictions by dynamical-photochemical models (Hourdin et al., 2004; Lavvas et al., 2008). Molecules showing a significant enhancement at northern latitudes are the nitriles (HC$_3$N, HCN) and the complex hydrocarbons (C$_4$H$_2$, C$_3$H$_4$). The D/H ratio on Titan was also determined from the CH$_3$D band at 8.6 micron and found to be about $1.17^{-0.16}_{-0.21} \times 10^{-4}$ (Coustenis et al., 2007), while Bézard et al. (2007) determined the D/H also from the CH$_3$D band, but adding the ^{13}CH$_3$D isotope and found it to be $1.32^{-0.15}_{-0.11} \times 10^{-4}$.

2. Observations in the FP3 and FP1 ranges

The CIRS instrument and its functions have been previously described (e.g. Flasar et al., 2004). It consists of three focal planes (FP) covering the range from 10 to 1500 cm^{-1}.

The 660–690 cm^{-1} region of Titan's spectrum of main interest here was recorded by the FP3 of CIRS (as part of the 600–1100 cm^{-1} range covered by this focal plane) and is very rich in spectral signatures (mainly emission bands originating in the stratosphere). From the molecules already known to exist on Titan, HC_3N, CO_2, and C_6H_6 have emission bands in this region, centered at 663, 667 and 674 cm^{-1} respectively. Furthermore, the low-frequency wing of the C_2H_2 band centered at 729 cm^{-1} significantly contributes here, as does, to a lesser amount, the R branch of the HCN band (centered at 713 cm^{-1}). All of these molecules had been included in our gaseous model (for a detailed description of the model see Coustenis et al., 2007). However, as already noted in that paper, an additional emission—unaccounted-for by the gas model—was observed near 678 cm^{-1} at all latitudes (Fig. 1). This extra emission was also previously noticed in ISO high-resolution data (Coustenis et al., 2003).

We performed spectral averages in the FP3 range as described in Coustenis et al. (2007) for different latitudes and for both high and medium resolution from CIRS data acquired during the three first years of observations (Tb-T23). These averages complement and improve on the ones listed in Table 2 of Coustenis et al. (2007), adding further spectral data. We furthermore created a very large (over 6000 spectra) average for the FP1 range.

The unidentified feature was monitored for latitudinal variations. Differences of limb averages taken in the northern latitudes with respect to mid-latitude and southern averages indicated the presence of a feature centered at 677.75 cm^{-1} which followed the observed acetylene intensities. It was therefore thought that it might well be an acetylene isotope.

The 678 cm^{-1} emission feature observed when the model was subtracted from the data at all latitudes (Fig. 1) was very closely compatible with the ν_5 emission band of C_2HD, as reported by Fusina et al. (2005). These authors reported another band, the ν_4, at 519 cm^{-1}.

In the spectrum shown in Fig. 2 we have highlighted a feature at 519 cm^{-1} that agrees well in position with the ν_4 Q-branch of C_2HD from the Fusina et al. paper. The HC_3N Q-branch also appeared on this same figure providing a sanity check. On this same spectrum the features appearing at 510 and 538 cm^{-1} are due respectively to a mylar feature (these are weak absorption bands in the spectrum of the mylar substrate on which the far-IR beamsplitter is mounted and which do not always calibrate out completely) and a 1/2-Hz spike. These features illustrate the limits of our current spectral analysis capabilities in this spectral region. Although it is clear that an improved reference spectrum—on which simulations could be performed—is required before this feature can be properly analyzed, we find that the "integrated radiance" from the Fusina et al. paper ($\sim 10^{-8}$ W cm^{-2} sr^{-1}/cm^{-1} for this band), is quite compatible with the observations shown in Fig. 2.

3. Laboratory work

Band intensity determinations for the two bending modes ν_5 and ν_4 have already been performed by Eggers et al. (1955) and by Kim and King (1979) but the C_2HD samples used in those studies were not pure. Eggers and colleagues used a sample where less than two thirds of the total sample pressure is attributed to C_2HD, while the rest is composed of C_2H_2 and C_2D_2. In the study of Kim and King, the sample purity was even worse since C_2HD accounted for only 61.5% of the total pressure. Since the ν_5 band of acetylene (729 cm^{-1}) and acetylene-d1 (678 cm^{-1}) are partially overlapping,

as do the ν_4 band of C_2HD (519 cm^{-1}) and the ν_5 band of C_2D_2 (537 cm^{-1}), the integrated absorbance needs to be corrected for the contribution of C_2H_2 and C_2D_2 using an estimated mixing ratio. In the study by Kim and King, the estimated mixing ratios are respectively 0.295 and 0.09 for C_2H_2 and C_2D_2. Taking into account the ν_5 band intensities of acetylene and acetylene-d1, one can calculate that both Q-branches almost reach the same intensity. Even the ν_5 band of C_2D_2 will reach half the intensity of the ν_4 band of C_2HD. In such conditions, the overlap could easily introduce uncertainties in the band intensity determination. Consequently, we have undertaken new band intensity measurements of C_2HD.

Acetylene-d1 (C_2HD) was obtained from C/D/N Isotopes Inc. The enrichment measured by gas chromatography and mass spectrometry was 97%. The gaseous sample (1 bar in a 0.5 L sealed glass container) was transferred under vacuum and stored at liquid nitrogen temperature. IR spectra were obtained with a Bruker Equinox 55 FTIR spectrometer at 0.5 cm^{-1} resolution and averaged over 200 scans to obtain a 1000 S/N (RMS) in the transmission. The spectrometer was continuously flushed with nitrogen to limit and stabilize carbon dioxide and water vapor absorptions. An empty cell reference spectrum was measured before filling the gas cell at the desired pressure. We used a 10.6 m SPECAC white cell, filled by evaporating between 0.01 and 0.05 mbar of C_2HD. A first spectrum was recorded to check for the presence of impurities. The gas cell was then completed with 1000 mbar of nitrogen, to broaden the lines and avoid saturation.

A typical absorbance spectrum at 0.0245 mbar is shown in Fig. 3 and compared to a simulation using the line positions from Fusina et al. (2005). The presence of C_2H_2 is clearly detected at 729 cm^{-1}, overlapping the ν_5 band. From our spectral simulation of both bands we obtain a value of 3% acetylene in the acetylene-d1 sample, confirming the expected enrichment of the sample. The integrated band intensities for ν_5 and ν_4 were obtained from eight independent measurements performed at eight different pressures between 0.01 to 0.05 mbar. The pressures used for the determination of the intensities were corrected for the presence of C_2H_2. In addition, the intensity of the ν_5 acetylene band has been subtracted from the intensity of the ν_5 acetylene-d1 band. The results are presented in Table 1.

Our results are in relatively good agreement with the previous determinations but are systematically lower than the results by Kim and King (1979), by respectively 25 and 15% for ν_5 and ν_4 (see Table 1). This seems to indicate a systematic underestimation of the C_2HD contribution in their measured integrated absorbance.

In conclusion, we are quite confident in our intensity measurements because we have a sample of 97% purity and an improved resolution with respect to previous studies of integrated band intensities, hence avoiding practically all band overlaps.

4. Analysis of the data

We have performed radiative transfer simulations of Titan's spectrum in the 600–700 cm^{-1} spectral region using a line-by-line code that includes spectral emissions from all previously known molecules in this region, and adding C_2HD. We have used the thermal profiles for different latitudes as inferred by Achterberg et al. (2008) and described also in Coustenis et al. (2007).

4.1. Detection of acetylene-d1 from nadir data

Simulations to fit the spectra with and without C_2HD are shown in Fig. 4 for the ν_5 (678 cm^{-1}) band. The other C_2HD ν_4 band at 519 cm^{-1} could not be modeled accurately because the detection is of low signal-to-noise and the FP1 spectrum is an average over a wide range of emission angles and tangent heights. However, a comparison of the relative peak intensities of ν_4 and ν_5
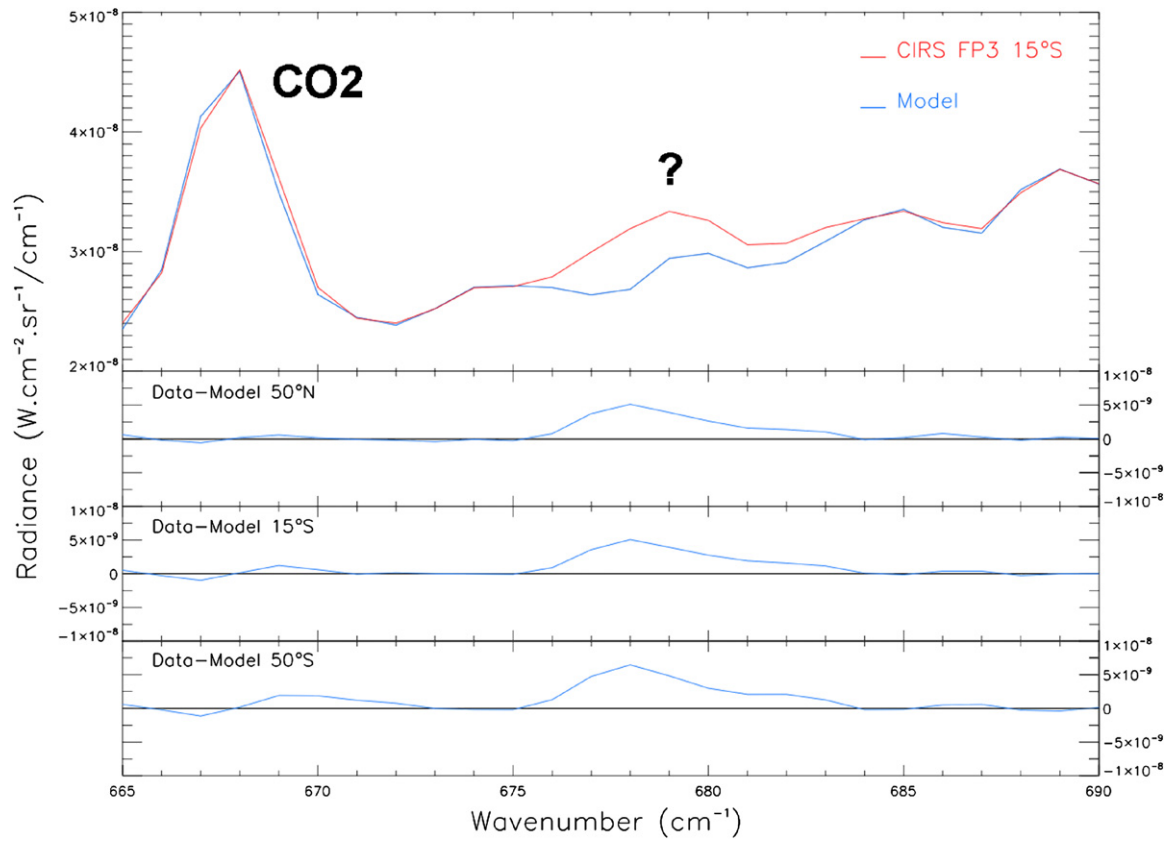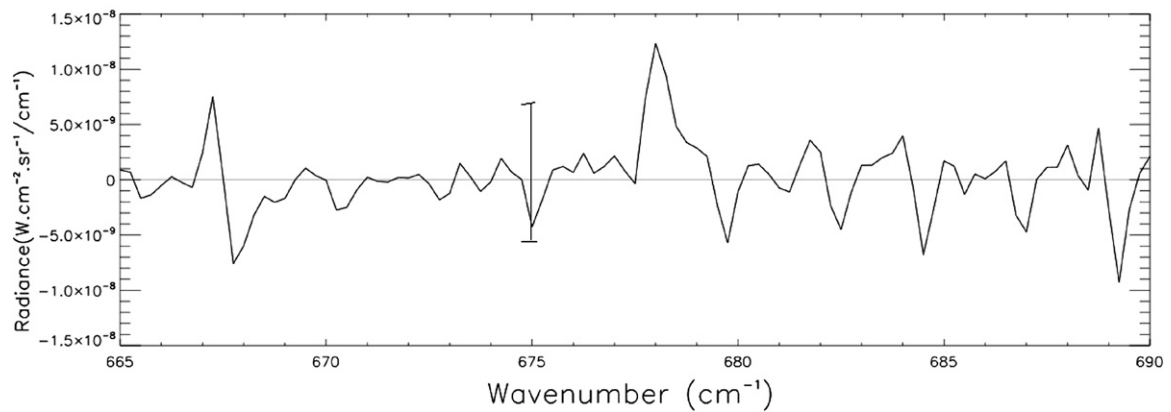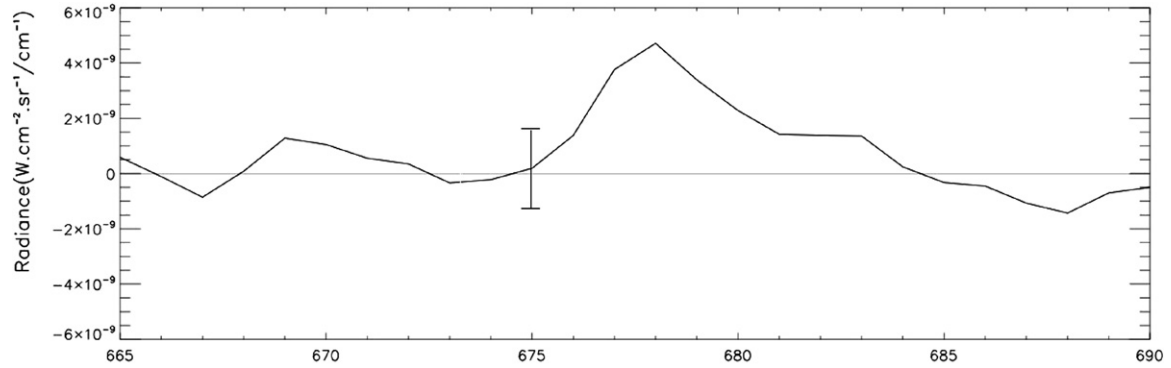
Fig. 1. (Upper panel) Excess emission observed (data−model) after fitting the CIRS spectra at three different latitudes at medium resolution (2.5 cm^{-1}). Although the model uses all known molecules, an unidentified emission remains at 678 cm^{-1} after a satisfactory fit of the rest of the spectral region is obtained. (Middle panel) The difference of data−model at medium resolution in unapodized spectra at 35° N also exposes the unidentified emission feature at 678 cm^{-1}; (lower panel) same as middle panel but for high resolution. 3-σ error bars are indicated. The averages contain several hundreds of spectra in general.
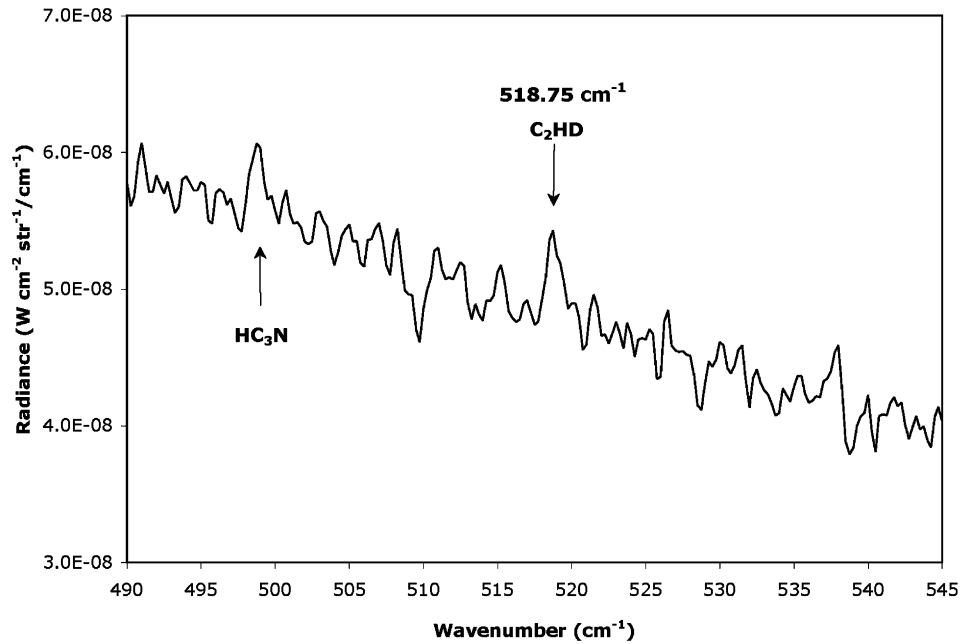
Fig. 2. Detection of C_2HD at 519 cm^{-1}. This figure shows the largest 0.5 cm^{-1} average we have been able to produce with the current dataset, showing the region around 519 cm^{-1}. This average covers 90° S to 90° N and includes both disk and limb spectra up to 300 km tangent height. The result contains 6838 spectra.
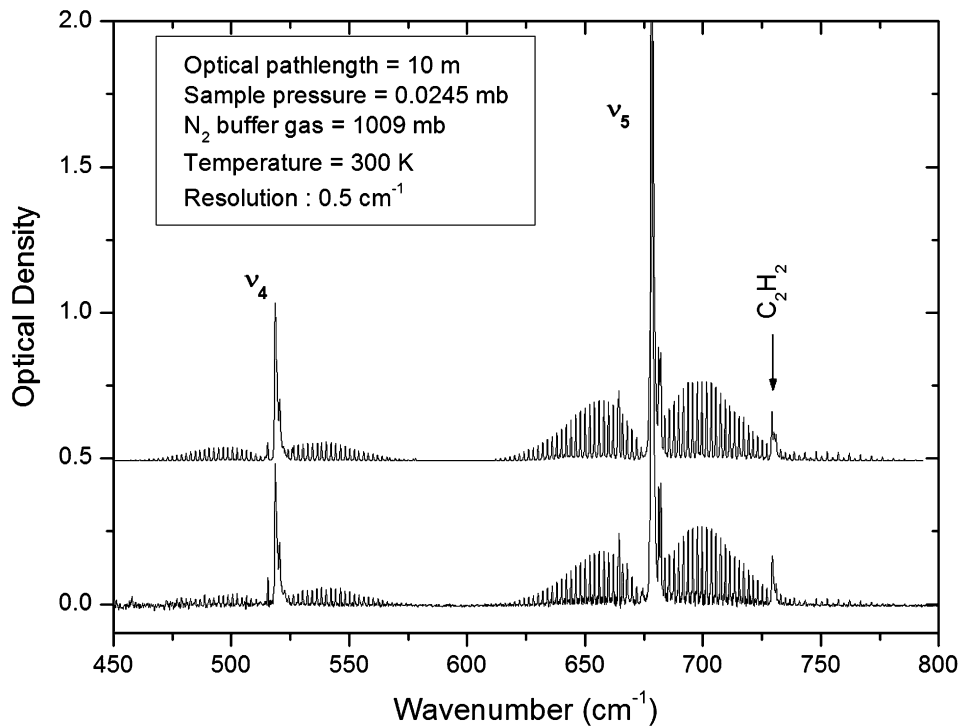

Fig. 3. Comparison between a typical laboratory spectrum (lower graph) and a simulation performed using line parameters of Fusina et al. (2005) with band intensities determined in the present work (upper graph, shifted by 0.5 for clarity). 3% of acetylene in the acetylene-d1 sample is introduced in the simulation to reproduce the experimental data.

Table 1
Comparison of the integrated band intensities in C_2HD

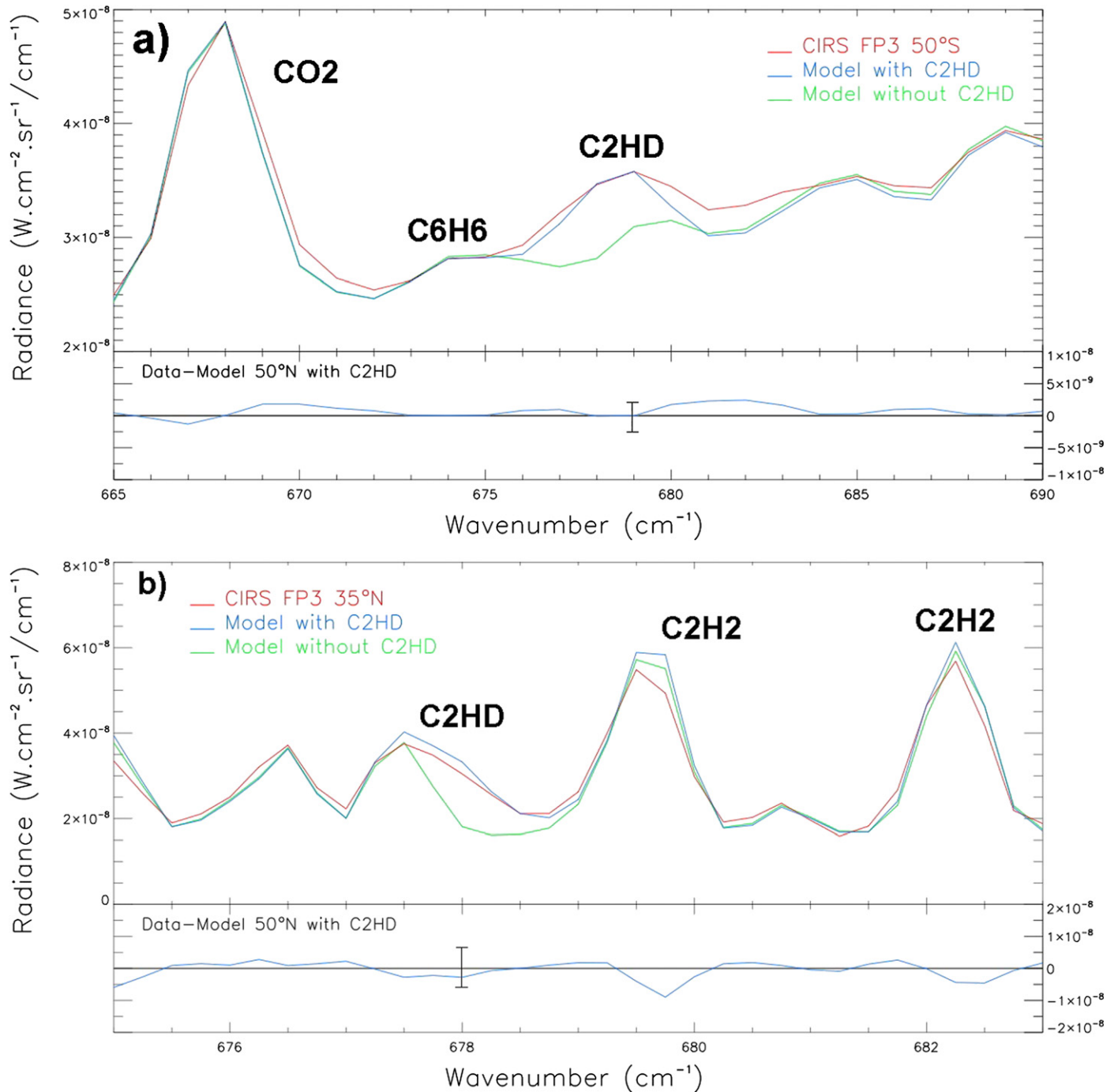| Band	Wavenumber (cm^{-1})	Intensities (cm at 296 K) Eggers et al. (1955)	Kim and King (1979)	This work
ν_5	678	$(1.39 \pm 0.25) \times 10^{-17}$	$(1.91 \pm 0.03) \times 10^{-17}$	$(1.40 \pm 0.05) \times 10^{-17}$
ν_4	519	$(3.2 \pm 0.6) \times 10^{-18}$	$(3.33 \pm 0.06) \times 10^{-18}$	$(2.88 \pm 0.17) \times 10^{-18}$

Fig. 4. (a) Simulated medium-resolution spectrum at 50° S with and without C_2HD. The emission band at 667 cm^{-1} is due to CO_2, while benzene (C_6H_6) contributes at 674 cm^{-1}. (b) High resolution CIRS data showing the fit obtained at 35° N with and without the C_2HD contribution which appears as a supplementary emission in the low-frequency wing of the 679.5 cm^{-1} C_2H_2 line. Other C_2H_2 lines are centered near 682.5, 685 and 689 cm^{-1}. Error bars are indicated at the 3-σ level.

in Titan with the measured laboratory intensities (Table 1) shows rough agreement and lends support to our identification of C_2HD in Titan.

4.2. The abundance of C_2HD and the D/H ratio in acetylene from nadir data

Using our radiative transfer code, we calculated the Titan spectrum in the 660–690 cm^{-1} region and iterated until we matched the Titan nadir observations at different latitudes, as shown in Fig. 4. This was achieved with the latitudinal abundances for CO_2, C_2H_2, HC_3N and C_6H_6 as indicated in Coustenis et al. (2007). When

the best fit was obtained, after several iterations, for the continuum and the near-by bands, we retrieved the abundance for C_2HD, using either a mixing ratio constant with altitude or a vertical distribution (as described in Coustenis et al., 2007, and Vinatier et al., 2007a) homothetic to the one used for the C_2H_2 band at 729 cm^{-1}. The latter approach yielded better fits in general (Coustenis et al., 2007). The ratio of the C_2HD/C_2H_2 abundances was retrieved individually at each latitude and allowed for the determination of the D/H ratio.

The C_2HD contribution functions at 678 cm^{-1} all peak around 6 mbar for nadir data at all latitudes, similarly to the 720 cm^{-1} C_2H_2 line, while the Q-branch of the acetylene band peaks near
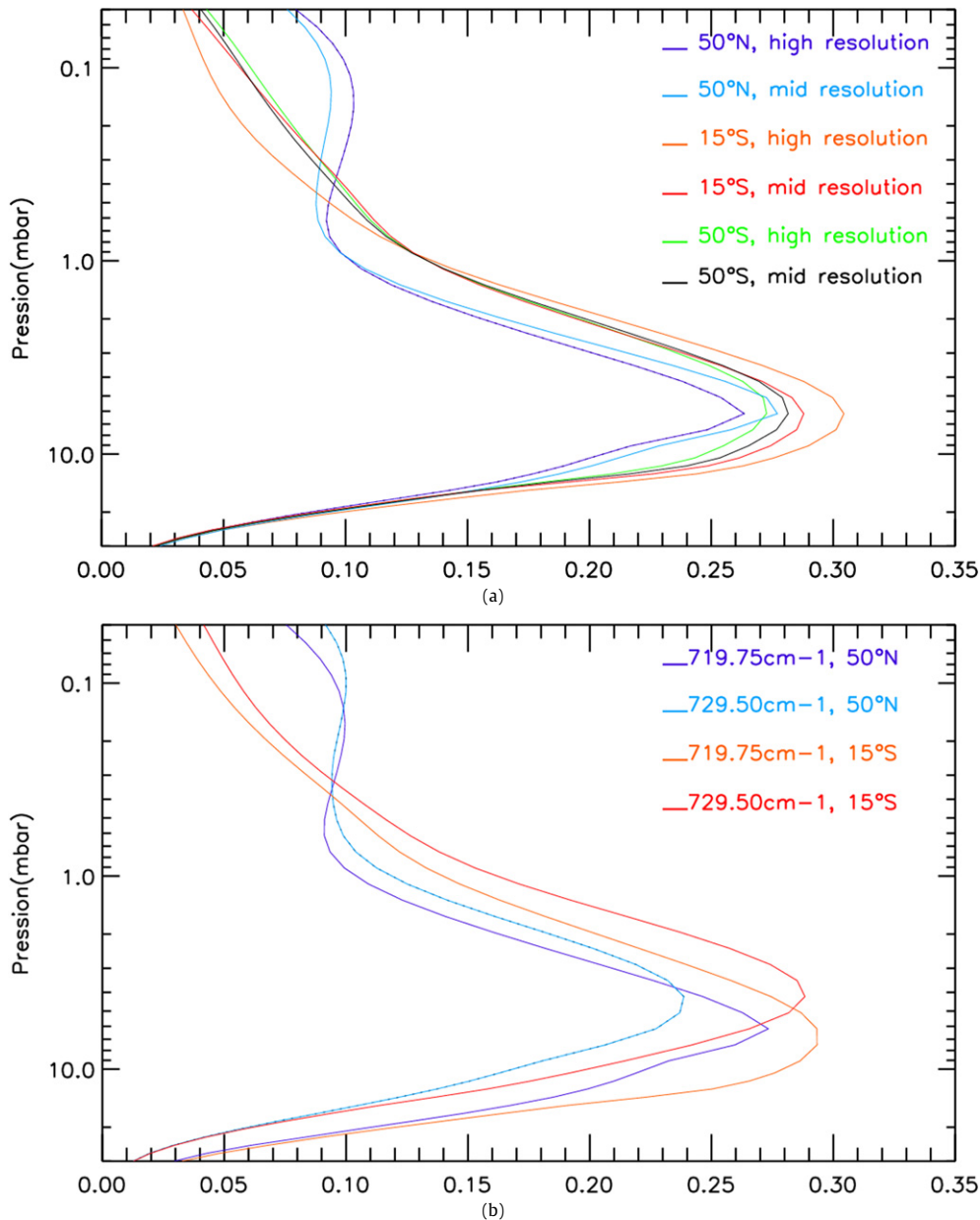
Fig. 5. Contribution functions of C_2HD at different resolutions and latitude points (a) all peaking around 6 mbar; and two lines of C_2H_2 (b) at two different latitudes at high resolution, peaking at somewhat higher altitude levels.

4 mbar (Fig. 5), at somewhat higher altitudes. When we divided the C_2HD and C_2H_2 abundances to infer the D/H ratios, we therefore used the acetylene abundances inferred not in the center but in the wings of the C_2H_2 band, at altitudes similar to the ones probed by C_2HD.

We find the C_2HD abundance at atmospheric levels around 6 mbar to be $1.27^{-0.13}_{-0.22} \times 10^{-9}$ from the nadir observations between the South pole and 45° N, which amounts to $\sim 3 \times 10^{-4}$ times the abundance of C_2H_2 at the equator. At latitudes higher than 60° N, a twofold increase of the C_2HD abundance is found, as is the case for acetylene (Coustenis et al., 2007). The D/H values we have inferred here are more accurate for mid-latitudes (33° S–33° N), where a maximum of nadir spectra are available in the spectral averages (8000–22,000) and the temperature profiles are more reliable. The weighted mean of the values of the D/H ratio, determined from the C_2HD/C_2H_2 ratios found in the different nadir latitude data and using the method described by Bevington (1969), is $2.09 \pm 0.45 \times 10^{-4}$. The full extents 1-$\sigma$ error bars include uncertainties on the thermal profile, the spectral calibration, the spectroscopic parameters, etc. (as described in Coustenis et al., 2007), but are mainly due to the lack of a precise determination of the vertical profile that perfectly matches the emission observed in the center and in the wings of the 729 cm^{-1} C_2H_2 band. We hope to have improved acetylene vertical distributions for all latitudes in the future. In the present case we used adjusted vertical profiles from Crespin et al. (2008), Vinatier et al. (2007a, 2007b) and from the Rannou et al. (2005, www.lmd.jussieu.fr/titanDbase) database and updates.

4.3. The limb data inferences

We additionally used limb and nadir data simultaneously in order to test a potential vertical variation of the D/H ratio. We used the spectral range 660–690 cm^{-1}, which also includes the spectral signatures of CO_2, HC_3N, C_6H_6 and C_2H_2. The vertical abun-
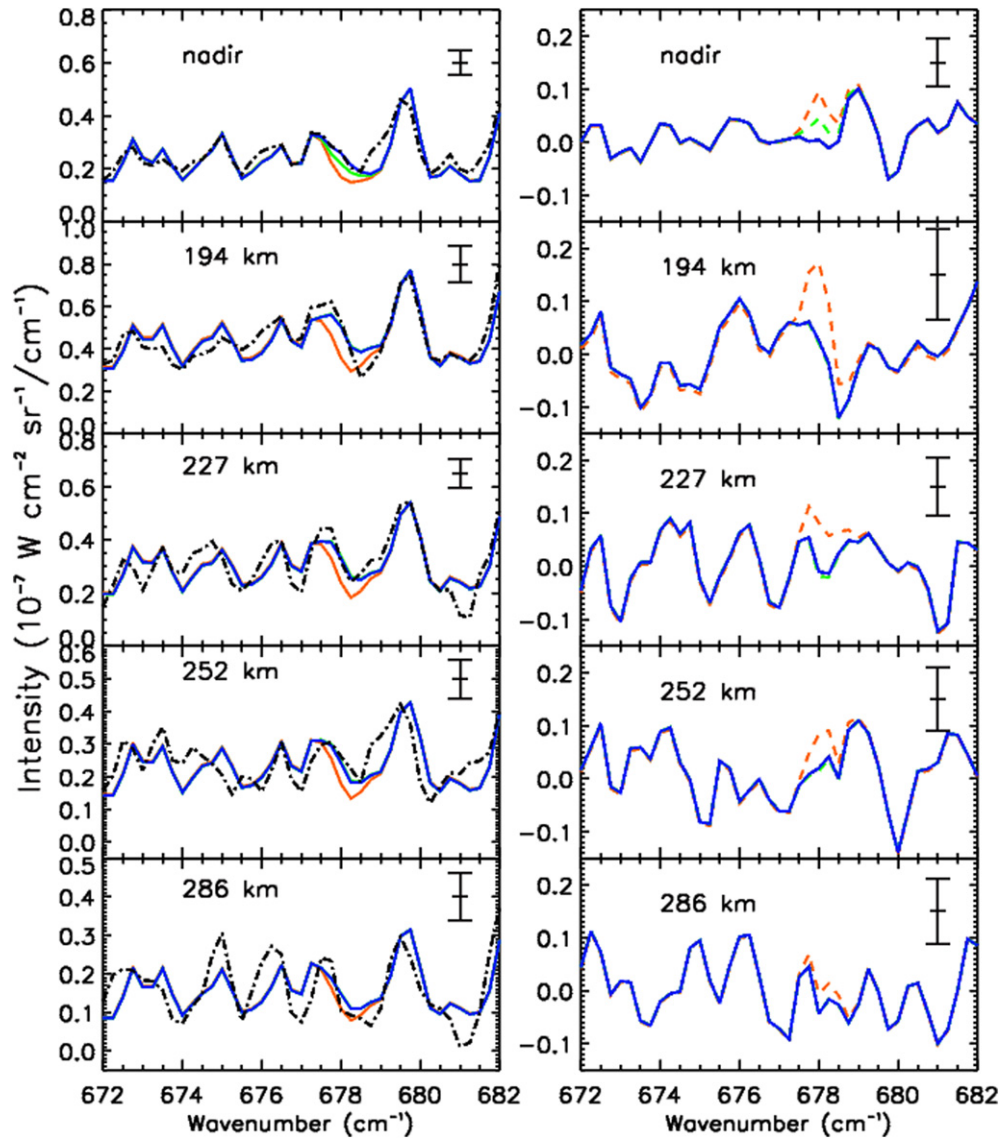
Fig. 6. (Left) Comparison between the observed spectra (dotted black line) at 54° S and the calculated spectra without (orange) and with emission of C_2HD corresponding to (i) an abundance profile homothetic to the C_2H_2 one (green) and (ii) with a C_2HD abundance profile retrieved with L = 3 (blue). (Right) Corresponding residuals with the C_2HD emission included in the calculations (green and blue) and without (orange). In green: the C_2HD abundance profile is homothetic to the C_2H_2 one; in blue: the C_2HD profile is retrieved with L = 3 (see text for details). The blue and green curves are almost superimposed at all wavenumbers excepted for the nadir around 678 cm⁻¹. The difference does not exceed the 1-σ level. The error bars are given at the ±1-σ level.

dance profiles of these latter molecules were retrieved previously (Vinatier et al., 2007a, 2007b).

We focus here on four latitudes: 54° S, 15° S, 54° N and 80° N. We used four limb spectral selections acquired during T15 (54° S), Tb (15° S), T10 (54° N) and T3 (80° N) flybys, all having a vertical resolution of about 30 km, except for T3 (50 km resolution). The altitudes of the line of sight of the limb spectra used in the retrievals are 194, 227, 252 and 286 km at 54° S; 242, 278, 314 and 349 at 15° S; 201, 237, 273 and 309 at 54° N and 166, 200 km at 80° N. Additionally, in order to constrain lower levels for the three mid-latitude selections, we simultaneously used three averaged nadir spectra recorded at comparable latitudes in the retrievals. The first selection, at 54° S, contains 883 spectra with a mean emission angle of 28°; at 15° S, the nadir averaged spectrum includes 3054 spectra with a mean emission angle of 32°, both selections were acquired between Tb and T20 flybys. Finally at 54° N, we used a nadir selection comprised of 14 spectra acquired during the T10 flyby with a mean emission angle of 55°. We did not use a nadir averaged spectrum in the retrieval of the

abundance profiles at 80° N because it does not probe lower levels than those probed by limb emissions, due to the low temperatures in the lower stratosphere.

The vertical temperature profiles at these four latitudes were previously retrieved by modeling the ν_4 CH₄ band at 1304 cm⁻¹ and incorporated in the retrieval process.

Fig. 6 shows the detection of C_2HD at 54° S on the nadir and several limb spectra by comparison between the observed spectra (dotted black lines), the calculated spectra with (blue and green) and without (orange) the C_2HD emission. We note that the detection of C_2HD in the nadir spectrum and on the two lowest-altitude limb spectra is clear but does not rise above the 2-σ level.

At these four latitudes, the vertical abundance profiles of C_2HD were first retrieved with a vertical correlation length of 3 scale heights (L = 3) and implied some slight variations of the D/H ratio with altitude, a trend which is questionable given the error bars on the retrieved abundance profiles of the isotope. The C_2HD abundance profile retrieved at 54° S with L = 3 is displayed in Fig. 7a as a solid black line and the corresponding calculated spectra are
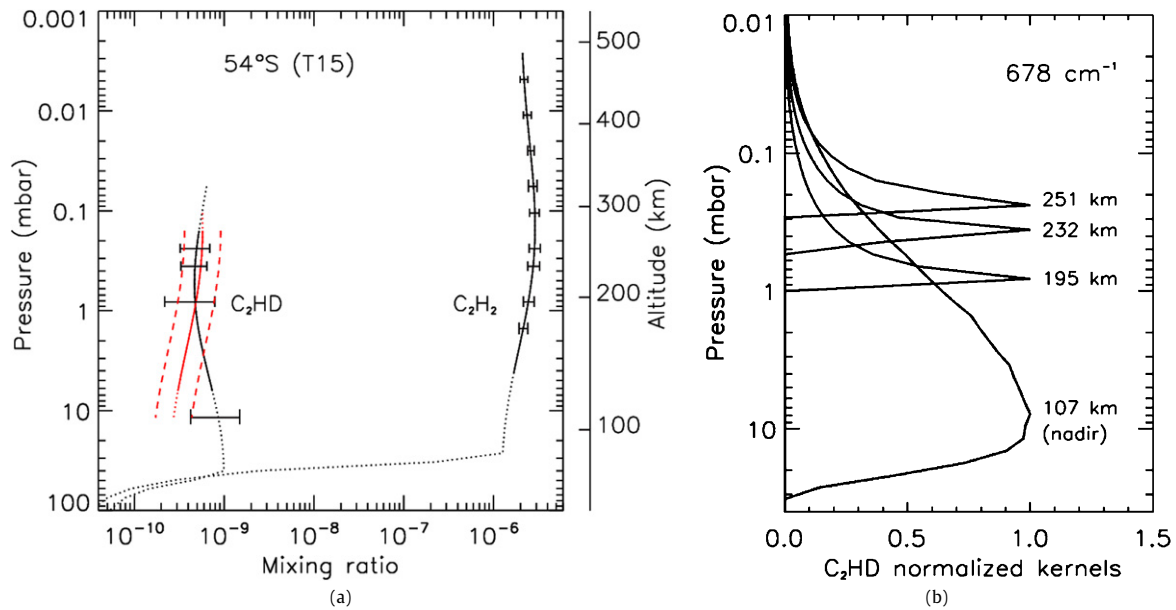
Fig. 7. (a, left) Retrieved abundance profiles of C_2H_2 and C_2HD at 54° S. The C_2HD black profile was retrieved with a correlation length of 3 scale heights (L = 3) whereas the red profile is homothetic to the C_2H_2 one (yielding a constant D/H ratio with altitude). Parts of the profiles displayed as dotted lines are not constrained by the observations. Error bars are given at the maxima of the kernels of the black C_2HD profile whereas an error envelop, displayed in dashed lines, shows the uncertainties of the red C_2HD profile. Both error bars correspond to the ± 1-σ level. (b, right) Normalized kernels calculated at 678 cm^{-1} at 54° S for the nadir and three limb emissions, corresponding to the C_2HD retrieved abundance profile homothetic to the C_2H_2 one (displayed in red on (a)). Altitudes are given at the kernel maxima. (For interpretation of the references to color in this figure legend, the reader is referred to the web version of this article.)
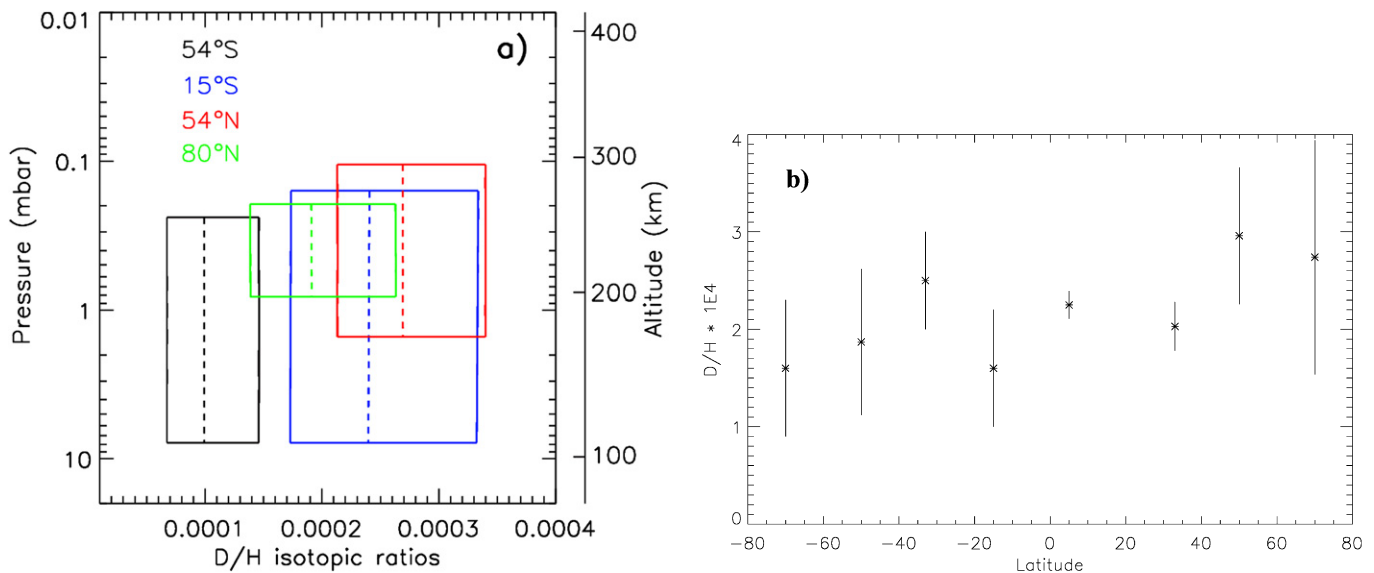

Fig. 8. (a, left) D/H isotopic ratios deduced at 54° S (black), 15° S (blue), 54° N (red) and 80° N (green). Mean values are given as dotted lines and ± 1-σ error envelopes are indicated as solid lines. Altitude scale refers to the 15° S latitude. (b, right) Examples at certain latitudes of D/H retrievals from nadir data.

displayed in Fig. 6a in a blue line. By forcing the D/H ratios to be constant with altitude, we then retrieved a C_2HD abundance profile (Fig. 7a, solid red line) that satisfactorily reproduces the observed spectra (nadir and limb, see Fig. 6a, green spectra). At the four latitudes, the differences between the spectra calculated with a L = 3-C_2HD retrieved profile and the C_2HD profile homothetic to the C_2H_2 one did not exceed the ± 1-σ level. We therefore constrained the D/H ratio to be constant with height at all latitudes.

Fig. 7b displays the normalized inversion kernels corresponding to the 678 cm^{-1} emission at 54° S for the nadir geometry (large kernel) and for the 3 deepest limb spectra (with lines-of-sight intercepting altitudes at 195, 232 and 251 km). As explained

in Vinatier et al. (2007a, 2007b) the inversion kernels represent the derivative of the ith intensity with respect to the logarithm of the mole fraction at grid level j (see that paper for the description of a kernel). Levels where kernels reach their maxima are correspondingly where the retrieved profiles are the most constrained by the observed spectra.

Fig. 8a displays the retrieved D/H ratios (dotted lines) at 54° S (black), 15° S (blue), 54° N (red) and 80° N (green), with the envelope error bars corresponding to the ± 1-σ deviation from the mean value (dashed line), and the altitude range probed by the spectra.

At 54° S, we retrieve $D/H = 9.6^{-4.5}_{-3.1} \times 10^{-5}$; at 15° S $D/H = 2.4^{-0.9}_{-0.7} \times 10^{-4}$; at 54° N $D/H = 2.7^{-0.7}_{-0.6} \times 10^{-4}$ and at 80° N, $D/H = 1.9^{-0.7}_{-0.5} \times 10^{-4}$.

We have made an average of these four values using the formulae from Bevington (1969) for performing weighted means of experimental measurements. We find the mean value to be $1.63 \pm 0.27 \times 10^{-4}$. Considering the large error bars (given for the ± 1-σ level), the values we retrieved at 54° S, 15° S, 54° N and 80° N are then consistent. The values inferred from the limb data are compatible with those retrieved from the nadir data. Examples of the latter are given in Fig. 8b.

5. Conclusions and interpretation

We report here the first detection of mono-deuterated acetylene (acetylene-d1, C_2HD) in Titan's atmosphere through the presence of two of its emission bands at 678 and 519 cm^{-1} observed in CIRS spectral averages of nadir and limb observations. We find the C_2HD value $(1.27^{-0.13}_{-0.22} \times 10^{-9})$ to be roughly constant with latitude from the South to about 45° N and then to exhibit a certain increase (by a factor of at most 2) in the North, as is the case for C_2H_2.

Fitting the 678 cm^{-1} ν_5 band simultaneously with the nearby C_2H_2 729 cm^{-1} ν_5 band, allowed us to infer a D/H ratio in acetylene with a weighted mean of $2.09 \pm 0.45 \times 10^{-4}$ and $1.63 \pm 0.27 \times 10^{-4}$ from nadir and limb data respectively, which both indicate a higher D/H ratio in acetylene than in methane. The high uncertainties mean that we do not at this time have the best possible precision, but that should improve in the future when a larger number of high-resolution spectra become available, in particular for the FP1 range where we detect the second C_2HD band, or at high northern latitudes.

The D/H ratio has also been determined in methane from CIRS data (Coustenis et al., 2007). That value (about 1.2×10^{-4}) is in good agreement with the one reported later by Bézard et al. (2007), who first included the $^{13}CH_3D$ isotope in their calculations $(1.32^{-0.15}_{-0.11} \times 10^{-4})$. The D/H value reported from measurements by the Huygens gas chromatograph mass spectrometer (GCMS) in hydrogen is $2.3 \pm 0.5 \times 10^{-4}$, significantly higher than that found in CH_3D (as discussed in Coustenis et al., 2007). This may indicate that the D/H measured by the GCMS (Niemann et al., 2005) is the value $HD/2H_2$ resulting from the photodissociation of methane.

Deuterated species in Titan's atmosphere have been detected in methane, hydrogen and as reported here for the first time, in acetylene. It has been recognized for many years now that the main reservoir of deuterium in Titan's atmosphere is in methane. The D/H ratio in this molecule has been subsequently found to be enriched with respect to the abundance in hydrogen in the solar nebula for reasons that are still controversial (see for instance Lunine and Tittemore, 1993).

Methane is dissociated by UV radiation and electrons so that it should have disappeared in a few tens of millions of years (Yung et al., 1984; Wilson and Atreya, 2004). It must therefore be replenished from an appropriate source, and Tobie et al. (2006) suggested that it could have been episodically outgassed from the interior of Titan. However, the question of the origin of methane present in the interior of the satellite remains, and several theories exist today.

One scenario invokes that methane was trapped in planetesimals produced in the Solar Nebula and embedded in the feeding zone of Saturn (Hersant et al., 2008). These planetesimals subsequently formed Titan, where, we speculate, methane is today present totally in the form of clathrate hydrates concentrated at the top of the subsurface ocean of liquid water. In another scenario, Atreya et al. (2006) consider that the planetesimals that

formed Titan incorporated silicates, water and carbon dioxide. On the Earth, hydrolysis of ultramafic silicates produces hydrogen, whose reaction with carbon dioxide would have produced methane. Atreya et al. (2006) suggest that this serpentinization process occurs on Titan and produces methane in its interior.

Future experiments may allow us to discriminate between the two scenarios:

In the first scenario, D/H in CH_4 is the relic of the value in methane embedded in the solar nebula at the time of the production of the planetesimals which formed Titan.

The second scenario (Atreya et al., 2006) implies that D/H in Titan is identical to that in water. D/H in H_2O has been measured in comets of the cloud of Oort and found to be about twice as large as than the value in CH_4 in Titan. In order to fit the Titan value, we would have to consider some isotopic exchange which would have occurred in the solar nebula between H_2O and the proto-solar H_2. Hersant et al. (2001) have calculated the distribution of D/H in water (and in HCN) throughout the nebula. These calculations fit values observed in three comets of the Oort cloud, but the value calculated at 10 AU is not consistent with the value in CH_4 in Titan. One possibility is that this exchange occurred in a warm subnebula, which has not been modeled so far. Future measurements of D/H in water ice deposited at the surface of Titan would be of major importance.

This theory of the methane origin can be addressed through a precise measurement of the D/H ratio in the interior, and also in comets. Although CH_4 has been detected in eight comets, and D/H measured in several species, the D/H ratio in methane has not been measured because CH_3D has not been detected so far.

Whatever the origin of methane, the question remains as to the apparently larger enrichment found here in D/H in C_2H_2 with respect to CH_4. The photodissociation of CH_4 in Titan's upper atmosphere produces H_2 (HD) and C_2H_2 (C_2HD). Subsequent photolysis may then enrich dihydrogen and acetylene with deuterium, compared to methane. This is because, when either CH_3D or C_2HD is photolyzed there is a preference for H atoms being removed over D atoms, and therefore we expect that the D/H ratio would be higher for the photochemical products—C_2HD and HD—than for the progenitor CH_3D. This is one option, supported by observations. D/H is enriched on Titan relative to the protosolar or jovian value (in hydrogen) $(2.35 \pm 0.3 \times 10^{-5}$, average of reported values, see Coustenis et al., 2007, for details). It varies in Titan from factors of about 4–7 for D/H in methane and 7–14 for the D/H in hydrogen (as noted in Nixon et al., 2008), and we now report an intermediate enrichment for acetylene (8–10). Note, however, that other mechanisms that can change the D/H ratio, include magmatic/cryovolcanic processes, escape, resupply, etc. In addition, there may be other sources of hydrogen than just photochemistry of CH_4, so that the D/H derived by the Huygens GCMS from hydrogen or that from C_2HD is not necessarily indicative of the fractionation in the methane photochemical process.

In summary, bearing in mind the large uncertainty in our derived D/H values, we believe that the D/H from our C_2HD data differ from that from CH_3D, and that the difference can be attributed to the source of D. The D/H from the GCMS data on HD tends to agree with our result from C_2HD. This would tend to support our argument that photochemistry led to the fractionation, whereas this is not the case with the CH_3D. From that we speculate that the methane on Titan arrived as methane.

To further validate this hypothesis, laboratory measurements of the reaction rates of CH_2D and C_2D need to be performed. Furthermore, increasing the accuracy of our measurements should permit us to better model the fractionation mechanisms in the future. In addition, we would also like to determine this isotopic ratio in ethane if we can detect C_2H_5D in the CIRS data. Finally, in order to progress in our understanding of the isotopic ratios,

improved spectroscopic parameters for $^{13}CH_3D$, for C_2H_5D and for the propane bands in the region of 1000–1200 cm^{-1} would also be required.

Acknowledgments

References

Achterberg, R.K., Conrath, B.J., Gierasch, P.J., Flasar, F.M., Nixon, C.A., 2008. Titan's middle-atmospheric temperatures and dynamics observed by the Cassini Composite Infrared Spectrometer. Icarus 194, 263–277.

Atreya, S.K., Adams, E.Y., Niemann, H.B., Demick-Montelara, J.E., Owen, T.C., Fulchignoni, M., Ferri, F., Wilson, E.H., 2006. Titan's methane cycle. Planet. Space Sci. 54, 1177–1187.

Bevington, Ph.R., 1969. Data Reduction and Error Analysis for the Physical Sciences. McGraw–Hill, New York.

Bézard, B., Nixon, C.A., Kleiner, I., Jennings, D.E., 2007. Detection of $^{13}CH_3D$ on Titan. Icarus 191, 397–400.

Coustenis, A., Salama, A., Schulz, B., Ott, S., Lellouch, E., Encrenaz, T., Gautier, D., Feuchtgruber, H., 2003. Titan's atmosphere from ISO mid-infared spectroscopy. Icarus 161, 383–403.

Coustenis, A., Achterberg, R., Conrath, B., Jennings, D., Marten, A., Gautier, D., Bjoraker, G., Nixon, C., Romani, P., Carlson, R., Flasar, M., Samuelson, R.E., Teanby, N., Irwin, P., Bézard, B., Orton, G., Kunde, V., Abbas, M., Courtin, R., Fouchet, Th., Hubert, A., Lellouch, E., Mondellini, J., Taylor, F.W., Vinatier, S., 2007. The composition of Titan's stratosphere from Cassini/CIRS mid-infrared spectra. Icarus 189, 35–62.

Crespin, A., Lebonnois, S., Vinatier, S., Bézard, B., Coustenis, A., Teanby, N.A., Achterberg, R.K., Rannou, P., Hourdin, F., 2008. Diagnostics of Titan's stratospheric dynamics using Cassini/CIRS data and the 2-dimensional IPSL Circulation Model. Icarus, in press.

Eggers, D., Hisatsune, I., van Halten, L., 1955. Bond moments, their reliability and additivity: Sulfur dioxide and acetylene. J. Phys. Chem. 59, 1124–1129.

Flasar, F.M., Kunde, V.G., Abbas, M.M., Achterberg, R.K., Ade, P., Barucci, A., Bézard, B., Bjoraker, G.L., Brasunas, J.C., Calcutt, S.B., Carlson, R., Césarsky, C.J., Conrath, B.J., Coradini, A., Courtin, R., Coustenis, A., Edberg, S., Edgington, S., Ferrari, C., Fouchet, T., Gautier, D., Gierasch, P.J., Grossman, K., Irwin, P., Jennings, D.E., Lellouch, E., Mamoutkine, A.A., Marten, A., Meyer, J.P., Nixon, C.A., Orton, G.S., Owen, T.C., Pearl, J.C., Prangé, R., Raulin, F., Read, P.L., Romani, P.N., Samuelson, R.E., Segura, M.E., Showalter, M.R., Simon-Miller, A.A., Smith, M.D., Spencer, J.R., Spilker, L.J., Taylor, F.W., 2004. Exploring the Saturn system in the thermal infrared: The composite infrared spectrometer. Space Sci. Rev. 115, 169–297.

Flasar, F.M., Achterberg, R.K., Conrath, B.J., Gierasch, P.J., Kunde, V.G., Nixon, C.A., Bjoraker, G.L., Jennings, D.E., Romani, P.N., Simon-Miller, A.A., Bézard, B., Coustenis, A., Irwin, P.G.J., Teanby, N.A., Brasunas, J., Pearl, J.C., Segura, M.E., Carlson, R., Matmoukine, A., Schinder, P.J., Barucci, A., Courtin, R., Fouchet, T., Gautier, D., Lellouch, E., Marten, A., Prangé, R., Vinatier, S., Strobel, D.F., Calcutt, S.B., Read, P.L., Taylor, F.W., Bowles, N., Samuelson, R.E., Orton, G.S., Spilker, L.J., Owen, T.C., Spencer, J.A., Showalter, M.R., Ferrari, C., Abbas, M.M., Raulin, F., Edgington, S., Ade, P., Wishnow, E.H., 2005. Titan's atmospheric temperatures, winds, and composition. Science 308, 975–978.

Fusina, L., Cané, E., Tamassia, F., Di Lonardo, G., 2005. The infrared spectrum of $^{12}C_2HD$: The bending states up to $\nu_4 + \nu_5 = 3$. Mol. Phys. 103, 3263–3270.

Hersant, F., Gautier, D., Huré, J.-M., 2001. A two-dimensional model for the primordial nebula constrained by D/H measurements in the Solar System: Implications for the formation of giant planets. Astrophys. J. 554, 391–407.

Hersant, F., Gautier, D., Tobie, G., Lunine, J.I., 2008. Interpretation of the carbon abundance in Saturn measured by Cassini. Planet. Space Sci. 56, 1103–1111.

Hourdin, F., Lebonnois, S., Luz, D., Rannou, P., 2004. Titan's stratospheric composition driven by condensation and dynamics. J. Geophys. Res. 109 (E1205). 15 pp.

Kim, K., King, W.T., 1979. Integrated infrared intensities in HCCH, DCCD and HCCD. J. Mol. Struct. 57, 201–207.

Lavvas, P.P., Coustenis, A., Vardavas, I.M., 2008. Coupling photochemistry with haze formation in Titan's atmosphere. Part II. Results and validation with Cassini/Huygens data. Planet. Space Sci. 56, 67–99.

Lunine, J.I., Tittemore, W.C., 1993. Origins of outer-planet satellites. In: Levy, E.H., Lunine, J.I. (Eds.), Protostars and Planets III. Univ. of Arizona Press, Tucson, AZ, pp. 1149–1176.

Niemann, H.B., Atreya, S.K., Bauer, S.J., Carignan, G.R., Demick, J.E., Frost, R.L., Gautier, D., Haberman, J.A., Harpold, D.N., Hunten, D.M., Israel, G., Lunine, J.I., Kasprzak, W.T., Owen, T.C., Paulkovich, M., Raulin, F., Raaen, E., Way, S.H., 2005. The abundances of constituents of Titan's atmosphere from the GCMS instrument on the Huygens probe. Nature 438, 779–784.

Nixon, C.A., Achterberg, R.K., Vinatier, S., Bézard, B., Coustenis, A., Teanby, N.A., de Kok, R., Romani, P.N., Jennings, D.E., Bjoraker, G.L., Flasar, F.M., 2008. The $^{12}C/^{13}C$ ratio in Titan hydrocarbons from Cassini/CIRS infrared spectra. Icarus 195, 778–791.

Rannou, P., Lebonnois, S., Hourdin, F., Luz, D., 2005. Titan atmosphere database. Adv. Space Res. 36, 2194–2198.

Teanby, N.A., Irwin, P.G.J., de Kok, R., Vinatier, S., Bézard, B., Nixon, C.A., Flasar, F.M., Calcut, S.B., Bowles, N.E., Fletcher, L., Howett, C., Taylor, F.W., 2007. Vertical profiles of HCN, HC_3N and C_2H_2 in Titan's atmosphere derived from Cassini/CIRS data. Icarus 186, 364–384.

Teanby, N.A., Irwin, P.G.J., de Kok, R., Nixon, C.A., Coustenis, A., Calcutt, S.B., Bowles, N.E., Fletcher, L., Howett, C., Taylor, F.W., 2008. Global variations of C_2H_2, C_3H_4, C_4H_2, HCN and HC_3N in Titan's stratosphere for early northern winter. Icarus 193, 595–611.

Tobie, G., Lunine, J.I., Sotin, C., 2006. Episodic outgassing as the origin of atmospheric methane on Titan. Nature 440, 61–64.

Vinatier, S., Bézard, B., Fouchet, T., Teanby, N.A., de Kok, R., Irwin, P.G.J., Conrath, B.J., Nixon, C.A., Romani, P.N., Flasar, F.M., Coustenis, A., 2007a. Vertical abundance profiles of hydrocarbons in Titan's atmosphere at 15° S and 80° N retrieved from Cassini/CIRS spectra. Icarus 188, 120–138.

Vinatier, S., Bézard, B., Nixon, C.A., 2007b. The Titan $^{14}N/^{15}N$ and $^{12}C/^{13}C$ isotopic ratios in HCN from Cassini/CIRS. Icarus 191, 712–721.

Wilson, E.H., Atreya, S.K., 2004. Current state of modeling the photochemistry of Titan's mutually dependant atmosphere and ionosphere. J. Geophys. Res. 103. E060002.

Yung, Y.L., Allen, M., Pinto, J.P., 1984. Photochemistry of the atmosphere of Titan: Comparison between model and observations. Astrophys. J. Suppl. 55, 465–506.